GENERATION MECHANISMS OF ZEBRA STRUCTURES IN SOLAR RADIO EMISSION ON THE BACKGROUND OF COMPLEX DYNAMIC SPECTRA

G. P. Chernov*, V. V. Fomichev**

N.V. Pushkov Institute of Terrestrial Magnetism, Ionosphere and Radio Wave Propagation RAS (IZMIRAN), Moscow, Troitsk, Russia

**e-mail: gchernov@izmiran.ru*

***e-mail: fomichev@izmiran.ru*

Received February 29, 2024

Revised May 01, 2024

Accepted July 25, 2024

Abstract. The discussion about the origin of the zebra structure has been going on for more than 50 years. In many papers it is usually postulated that the double plasma resonance mechanism always works if there are fast particles in the magnetic trap. Due to a number of difficulties encountered by this mechanism, works on its improvement began to appear, mainly in a dozen papers by Karlitsky and Yasnov, where the whole discussion is based on the variability of the ratio of the magnetic field and density height scales and the assumption of some plasma turbulence in the source. Here we show the possibilities of an alternative model of interaction of plasma waves with whistlers. Several phenomena were selected in which it is clear that the ratio of height scales does not change in the magnetic loop as the source of the zebra structure. It was shown that all the main details of the sporadic zebra structure in the phenomenon of 1 August 2010 (and in many other phenomena) can be explained within the framework of a unified model of zebra structure and radio fibers (fiber bursts) in the interaction of plasma waves with whistlers. The main changes in the zebra structure bands are caused by the scattering of fast particles on whistlers, leading to switching of the whistler instability from the normal Doppler effect to the anomalous one. In the end, the possibilities of laboratory experiments are considered and the solar zebra structure is compared with similar bands in the decametre radio emission of Jupiter.

DOI: 10.31857/S00167940250601e9

1. INTRODUCTION

Understanding the nature of the fine structure of the radio emission of solar radio bursts is one of the most important criteria to verify the radio emission mechanisms. The zebra structure (ZS) belongs to the most remarkable type of fine structure. It appears on dynamical spectra as regular bands in emission and absorption. It has been described in numerous papers and monographs, starting from the first publication by Elgarøy [Elgarøy, 1959; Kuijpers, 1975; Slottje, 1981; Chernov, 1976; 2006; 2011].

The discussion about the origin of the zebra structure has been going on for more than 50 years [Chernov, 2011]. The most frequently discussed mechanism is based on double plasma resonance (DPR) [Zheleznykov and Zlotnik, 1975a, b]:

$$\omega_{UH} = (\omega^2_{Pe} + \omega^2_{Be})^{1/2} = s\omega_{Be} ,$$

(1)

where ω_{Pe} – electron plasma frequency, ω_{Be}– electron gyro frequency under conditions where $\omega_{Be} << \omega_{(Pe)}$[Zheleznykov and Zlotnik, 1975a , b; Kuijpers, 1975; 1980; Mollwo, 1983; 1988; Winglee and Dulk, 1986]. These works usually postulate that the mechanism always works if there are fast particles in the magnetic trap. However, it encounters a number of difficulties in explaining the dynamics of the WL bands (abrupt changes in the frequency drift of the bands, a large number of harmonics, frequency splitting of the bands, and their ultrafine structure in the form of millisecond spikes). Therefore, works on both its improvement [Karlický et al., 2001; LaBelle et al., 2003; Kuznetsov and Tsap, 2007] and creation of new models began to appear.

In a dozen papers by Karlitsky and Yasnov, the method of estimating the number of harmonics was improved within the framework of the DPR, mainly towards its increase, bringing it to 170-200. At the same time, no comparisons with other models were made as a rule.

Here we note some of their important results with the involvement of their discussion in the framework of an alternative zebra model on whistlers.

2. COMPLEX ZEBRA-STRUCTURE SPECTRA

Fig. 1 and Fig. 2 show spectra of the zebra structure with different band parameters both with time and at different frequencies. Here, it is difficult to justify the mechanism on the DPR even for some parts of the spectrum, ignoring others.

Fig. 1.

Fig. 2.

Almost simultaneously with the DPR, an alternative mechanism for the interaction of plasma waves (l) with whistlers (w) was proposed, $l + w \rightarrow t$ [Chernov, 1976; 1990]. In this model, the above-mentioned subtle effects of the WL bands are explained by quasilinear effects of the interaction of fast particles with whistlers. The mechanism with whistlers became its natural development after its application by Kuijpers [Kuijpers, 1975] for fibers (fiber bursts), when in some phenomena a continuous transition of WG fringes into fibers and back was observed. The most important details of this mechanism are presented in the Discussion section.

In the seminal work on the DPR mechanism [Zheleznykov and Zlotnik, 1975a] it was shown that the relative width of the increment band in the hybrid band turns out to be incredibly narrow $\delta\omega/\omega_{Be}$~$2.5\text{-}10^{-4}$. Such a value is obtained only if the dispersion of the particle beam velocities is discarded as an infinitesimal quantity in the estimations. In [Benáček et al., 2017] it is shown that taking into account the velocity dispersion of hot particles and the cold plasma temperature severely limits the efficiency of the DPR mechanism. Then, Karlický and Yasnov contributed a lot to improve the mechanism on DPR in a dozen of their papers. In a recent paper [Yasnov and Karlický, 2020] made an important update in this endeavor. Following the paper [Yasnov and Chernov, 2020], they pointed out the importance in analyzing any phenomenon of taking into account the change in the ratio of the magnetic field and density variation scales at the source of the zebra-structure. For example, in [Yasnov and Chernov, 2020] this ratio was considered constant and the advantage of the whistler mechanism was shown for the 21.06.2011 phenomenon.

In the introduction of [Yasnov and Karlický, 2020], the authors mentioned all the main works on observations of the zebra structure and theoretical mechanisms to explain it (more than 20 papers), which obviates the need to repeat them here. They proposed an improved method for determining the gyroharmonics of zebra bands, which is essential for determining the electron density and magnetic field strength in the zebra source. Compared to previous methods, a new assumption is made that the ratio $R = L_{bh}/L_{nh}$ (where L_{bh} and L_{nh}− characteristic scales of magnetic field and density variation) vary in the source in a more generalized form. Almost free manipulation of the variability of R allows us to obtain for the 21.06.2011 phenomenon new values of gyrofrequency numbers around 115 (instead of 50-60 in [Yasnov and Chernov, 2020], and in other phenomena up to 170. This does not mention previous results of the authors [Benáček et al., 2017], where it is shown that in real parameters the amplitude of the cone instability increment drops significantly by the 30th harmonic.

This fact alone indicates the unsuitability of the proposed model improvement on the DPR, in particular, to determine the harmonic number of the zebra structure bands by manipulating the variability of the ratio of the ratio of the scales of magnetic field and density variations in both one phenomenon and different ones.

In previous work [Karlický, 2014] it was assumed that all frequency variations of zebra bands are caused by some kind of turbulence. Recent papers attribute everything to the propagation of a fast magnetosonic wave [Karlický, 2022], since there a strict period of fluctuations coinciding with the classical cosine function was determined. Interestingly, the August 17, 1998 phenomenon is analyzed once again, after first being considered in [Zlonik et al., 2009]. These are fast pulsations of zebra structure packets (similar to type III bursts) against a background of pulsations in absorption. [Zlonik et al., 2009] believed that two non-equilibrium distribution functions were present in the source: one with a cone velocity distribution, responsible for the continuum emission, and another of the Dory, Guest, and Harris type, capable of inducing the DPR effect by inducing a zebra structure. [Karlický, 2022] does not mention it. The DPR mechanism is assumed to work and the harmonic number at the lower frequency is determined using a newly developed method (mentioned above) for 13 zebra moments at different frequencies from 254 to 287 MHz. The maximum harmonic numbers are obtained at 270.6 MHz, $s1 = 177.6$ and at 268.6 MHz $s1 = 214.6$.

Such large unlikely harmonics stimulate recalling an alternative interpretation of this phenomenon. The review [Chernov, 2019] notes some properties on the spectrum with WL packets that have not been considered anywhere since [Zlotnik et al., 2009]. Not all WL packets have a negative frequency drift (like type III bursts). A number of moments with positive drift can be seen. WL is also visible between packets, and one can see continuous zebra stripes throughout the five packets with noticeable sawtooth frequency drift. Between the WL packets, the ripples in absorption have a varied frequency drift.

Similar spectra, with almost vertical zebra packets, have been observed in many phenomena, starting with the excellent example in Fig. 6 in [Slottje, 1972]. In the July 03, 1974 phenomenon, such zebra packets appeared for several hours [Slottje, 1972; Chernov, 1976]. Earlier we have already shown the advantage of the whistler model for interpreting the phenomenon of 21.06.2011. [Yasnov and Chernov, 2020]. Even earlier, a mechanism with whistlers based on the scattering of fast particles on whistlers was used to explain the sawtooth frequency drift of zebra stripes in the known phenomenon of 25.10.1994 [Chernov, 2005]. Whistlers are always generated simultaneously with plasma waves at the upper hybrid frequency by fast particles with a cone velocity distribution. The scattering process on whistlers was used in [Chernov, 1990] and in more detail in [Chernov, 1996; 2005]. There, an important property of the process was considered: the change in the direction of the frequency drift of zebra bands should correlate with the change in the direction of the spatial drift of their radio sources (see Fig. 2 in [Chernov, 2019]).

When fast particles scatter on whistlers, the distribution function changes, the generation of whistlers can switch repeatedly from the normal Doppler effect to the anomalous one. In [Zlotnik et al., 2003] for the 25.10.1994 phenomenon, a barometric formula is used to determine the temperature and select the magnetic loop. However, the concentration distribution according to the barometric formula cannot be applied in magnetic loops with plasma β << 1 because this formula gives the density distribution in the gravity field at constant temperature and without taking into account the magnetic field.

When fast particles scatter on whistlers, the distribution function changes, the generation of whistlers can switch repeatedly from normal Doppler effect to anomalous (fan instability).

If fast particles interact with whistlers at the cyclotron resonance

$$\varpi^{w} - k_{\|}v_{\|} - s\varpi_{Be} = 0 \qquad (2)$$

(at normal Doppler resonance s = +1), waves and particles are oppositely directed ($k_{\|}\, v_{\|} < 0$ or $\omega/k_{\|} < 0$) ($k_{\|}$ and $v_{\|}$– components of the wave vector and velocity parallel to the magnetic field), particles move along diffusion curves. When the maximum of the distribution function shifts toward larger $v_{\|}$, the anomalous Doppler effect is turned on (s = -1 in (1)). In these cases, the group velocity of whistlers changes sign to the opposite (smoothly or abruptly depending on the parameters of the fast particles). And as a result, the frequency drift of the bands synchronously changes to the reverse (see in detail in [Chernov, 1996]).

Karlitsky and Yasnov usually analyze phenomena with regular zebra bands, but more often the spectra are very complex with superposition not only of fast pulsations, but also with fiber bursts with different frequency drift, which are sometimes difficult to distinguish from WL (e.g., as in Figs. 1 and 2).

The whole discussion is based on the variability of the ratio of the magnetic field and density scales. Already this indicates difficulties for the model on the DPR. It is clear from the spectra of a number of phenomena that the ratio of the scales of change of field and density cannot change instantaneously in a loop.

Moreover, they use a number of known phenomena with a large number of bands without touching many other effects on the same spectrum. For example, ignoring the explanations for the sawtooth frequency spectrum of the bands, the connection with fast pulsations, abrupt transitions, jumps in band parameters at the same frequencies, and other points.

3. DISCUSSION

The application of the DPR mechanism is simply postulated. After a large review [Zheleznyakov et al., 2016], there is no need to repeat its description in detail now. It remains the most cited in analyzing the zebra structure. It is based on the generation of plasma waves at the upper hybrid frequency ω_{UH} by fast electrons with a velocity distribution function with a loss cone. Their subsequent transformation into electromagnetic waves generates continuum radiation, which can be sharply amplified at DPR levels where ω_{UH} is approximately equal to an integer number s of electron cyclotron harmonics ($\approx s\omega_{Be}$). This simple algebraic relation is the basis of the beautiful zebra structure theory (which has become almost classical) presented in [Zheleznyakov and Zlotnik, 1975a, b] and then supported in [Winglee and Dulk, 1986].

The basic condition for the existence of many DPR levels implies that the scale of magnetic field variation should be much smaller than the scale of density variation. However, this condition is shown in the listed works in the form of a hypothetical scheme without numerical scales on the axes, shown in Fig. *3a* as a fragment of Fig. 2 in the review [Zheleznyakov et al., 2016].

Fig. 3.

If we try to use for this purpose the known analytical expressions for the density and magnetic field dependence in the corona, no known models support the possibility of the formation of many levels of DPR in reasonable sizes of zebra structure sources. For illustrative purposes, see Figs. 6 and 7 in [Chernov, 2019] on page 217, raising doubts in general about the use of a model on DPR to explain the numerous zebra bands, even disregarding the many effects of complex band dynamics.

Fig. 4.

Fig. 4 shows the calculation of DPR levels using the usual (generally accepted) coronal plasma parameters using the barometric formula: electron temperature $Te = 1.2\cdot10^6$ K, initial plasma frequency f_{P0} = 3800 MHz at altitude h_{B0} = 20000 km. If the dipole dependence of the magnetic field is used for cyclotron harmonics, harmonics with $s \geq 50$ go to much higher altitudes ≥ 100000 km. Thus, excitation of waves simultaneously at 34 DPR levels in the corona is not feasible in any real density and magnetic field models. In recent works, Karlitsky and Yasnov proposed an exotic model (Fig. 3*b*) with a hump on a smooth density decline [Selhorst et al., 2008], on the steep slopes of which the DPR conditions must be fulfilled to generate a large number of harmonics [Yasnov et al., 2016].

Fig. 1 shows a spectrum of about 45 s duration with a complex zebra structure, but in the absence of regular bands it is difficult to find a moment where the mechanism on the DPR could be applied. The zebra structure is wedged into a broad band in absorption, against which a chain of narrow-band (rope-like) fibers develops [Chernov, 1997; 2008; Chernov et al., 2007].

In Fig. 2, the structure of the bands changes dramatically in 15 s the fibers (similar to fiber bursts) smoothly transform into zebra stripes with a wavy frequency drift. Obviously, the ratio of the scales of field and density changes cannot change appreciably in a few seconds.

Zebra spectra with sawtooth frequency drift of the bands were considered in [Karlický, 2014] using the spectra of Obs. Ondřejov in the decimeter band in the phenomenon of 01.08.2010. Without going into details, we note that the aim of the work was to show that within the DPR model the source zebra structure is in a turbulent state based on the analysis of the Fourier time profiles of the intensity of the bands with frequency (and from the relations $\omega_{UH} \approx \omega_{Pe}$ and $n_e \sim \omega^2{}_{Pe}$ and with the plasma density). The Fourier density fluctuation profile is taken as the calculated zebra band profile (apparently assuming that this does not require proof). The oscillation power spectrum has a steppe form with the index− 5/3, coinciding with the Kolmogorov spectrum for turbulence.

Independently of this work, it was shown in [Chernov et al., 2018] that all the main details of the sporadic zebra structure in the August 1, 2010 event can be explained within the framework of a unified model of the zebra structure and radio fibers in the interaction of plasma waves with whistlers (without strong plasma turbulence in the source). The main changes in the zebra structure fringes are caused by the scattering of fast particles on whistlers, leading to a switch of the whistler instability from the normal Doppler effect to the anomalous one.

3.1 Modeling of WL bands

In connection with the remark above about the impossibility of obtaining many DPR levels in any known density and magnetic field models (see Fig. 4), we can mention the work [Karlický, 2022] on modeling solar radio zebra bands. In fact, it is not modeling (simulation), but a fitting of the plasma parameters in the source to obtain model points on the zebra band on the spectrum coinciding with the observed ones, without calculating the radiation generation within the framework of the mechanism on the DPR, just plotting a graph like Fig. 4. And the main conclusion at the end confirms our conclusion (without reference), since the chosen field values do not coincide with any known models. There is also a business conclusion at the end: it is necessary to continue calculations of the increments of the upper hybrid waves for large harmonic numbers (in the paper s = 120-124).

In the spectrum of Fig. 2, a smooth transition of fibers (fiber bursts) into zebra bands with sawtooth frequency drift is visible at its beginning. The same transition or reverse transition was observed in the phenomenon 01.08.2010. Karlický [Karlický, 2014] does not discuss this effect, which is probably due to the fact that earlier in [Karlický, 2013] the model of fiber excitation on whistlers [Kuijpres, 1975] is rejected and a new, or tweaked model [Treumann et al., 1990] based on Alven solitons is proposed.

3.2 Explosive instability

The mechanism proposed in [Fomichev et al., 2009], which is based on the stabilization of explosive instability by cascading growth of ion-sound harmonics, turns out to be much more efficient than the mechanism of whistler instability on ion-sound harmonics. It provides a large number of sound harmonics with frequency separation independent of the ratio of plasma and cyclotron frequencies in the source and growing with frequency (in accordance with observations). No additional rigid conditions are imposed. The former condition of acceleration of mono-velocity beams of weakly relativistic particles, which is usually realized in any large flare, remains.

3.3 Laboratory experiments ([Viktorov et al., 2015])

Fig. 5.

To confirm the effectiveness of the DPR mechanism, one sometimes refers to perhaps the only work on the creation of radiation at the DPR in a laboratory plasma experiment [Viktorov et al., 2015]. Although now references to it are gradually quieting down [Chernov, 2019], since ambiguous results are demonstrated there (according to Fig. 5): the emission is fixed only in the form of complex bands at the second harmonic of the cyclotron frequency, while the experiment demonstrated the third harmonic as well (in Fig. 2). And if it were so easy to model, one would expect the experiment to be repeated many times, which would really be a proof of the mechanism's work. However, only the assurances of the authors that they seek to obtain radiation at the third harmonic were hearsay.

It is noteworthy that Viktorov et al. [2015] show in their experiment the simultaneous generation of whistlers at a frequency near 0.5 f_{ce} in Fig. 3b and complex shaped bands near frequency 2 f_{ce} in Figs. c and d, but the authors did not include these facts in the topic of their paper.

3.4 Zebra structure in Jupiter's decameter radio emission ([Panchenko et al., 2018])

Fig. 6.

Observations of the ZS similar in solar radio emission were carried out at the large ground-based radio telescope URAN-2 (Poltava, Ukraine) [Litvinenko et al., 2016]. The WL bands (see Fig. 6) are strongly polarized radio emission with durations from 20 to 290 s with a flux density of ~105-106 Jans (normalized to 1 a.u.), i.e., 1-2 orders of magnitude lower than for the decameter radio emission of its moon Io. The frequency splitting between the bands increases slightly with increasing emission frequency (in 43 events), typically between 0.5 and 1.5 MHz. In all examples, the bands exhibit rapid wavelike frequency drift while remaining quasi-distant from each other. All these facts are analogous to the solar WL.

Unlike the solar corona, Jupiter's plasma is strongly anisotropic, that is, $f_{pe} \ll f_{ce}$, in most regions of the magnetosphere. Therefore, the DPR mechanism with electrons cannot explain our observations because it requires extremely high plasma density, which is very unlikely in Jupiter's magnetosphere. [Zlotnik et al., 2016] proposed an alternative mechanism for the formation of the zebra structure in the kilometer-scale radiation of Jupiter. The model is based on DPR on ion cyclotron harmonics. The mechanism involves excitation of ion cyclotron waves at the lower hybrid frequency (f_{LH}), and then nonlinear transformation of this low-frequency emission into a high-frequency wave due to the process of merging with a high-frequency mode.

DPR with ions can operate in regions where $f_{pe} \ll f_{ce}$, which is fulfilled in most regions of Jupiter's magnetosphere. Therefore, the DPR effect on ion cyclotron harmonics can be realized at much lower plasma densities than the DPR effect on electron cyclotron harmonics. In this case, $f_{LH} \approx f_{pi}$ (f_{pi} is the ion plasma frequency), and the resonance condition is $f_{LH} = sf_{ci}$. Low-frequency plasma waves cannot escape from the source and must first be converted into high-frequency electromagnetic waves (f_{em}) in a nonlinear fusion process with a high-frequency mode (e.g., plasma waves at the upper hybrid frequency). The *fusion* of these waves ($f_{em} = sf_{ci} + f_{ce}$) leads to the generation of electromagnetic waves with a spectrum in the form of an EW. Nevertheless, additional theoretical studies are needed to clarify the nonlinear conversion of modes from low-frequency ion cyclotron waves to high-frequency electromagnetic waves.

4. PRELIMINARY CONCLUSIONS

A brief review of possible alternative excitation mechanisms for the zebra structure, in connection with the difficulties of the DPR mechanism noted in the Introduction, shows that the whistler mechanism and explosive instability (scattering of nonlinear ion-sonic waves on particles) can serve as possible models for simultaneous excitation of many zebra bands. They do not require any additional conditions (or constraints) on the plasma parameters.

Radio sources of fibers (fiber bursts) and WL in the whistler model must have moving sources, and the spatial drift of the WL bands must change synchronously with the change of the frequency drift on the dynamical spectrum. In the DPR model, the source of the WL should be rather stationary.

There are more developed theories, but there is no final decision on them. For example, propagation through a medium with inhomogeneities assumes their presence with certain scales [Laptuhov and Chernov, 2006; 2009]. An even more detailed analysis of zebra in Jupiter's radio emission is required.

The world network of CALLISTO radio telescopes does not yet allow us to use its spectra; almost 90% of them are subject to local interferences (interfirences), and the low frequency resolution of the pure spectra does not allow us to record the ZS bands.

ACKNOWLEDGEMENTS

The authors are grateful to the RHESSI, GOES, and LASCO spacecraft teams for open access to their data.

FUNDING

This work was supported by the Ministry of Education Science Project KP19-270.

REFERENCES

1. *Benáček J., Karlicky M., Yasnov L.V.* Temperature dependent growth rates of the upper-hybrid waves and solar radio zebra patterns // Astron. Astrophys. V. 598. ID A108. 2017. https://doi.org/10.1051/0004-6361/201629395

2. *Chernov G.P.* Microstructure in the continuous radiation of type IV meter bursts. Modulation of continuous emission by wave packets of whistlers // Sov. Astron. V. 20. N 5. P. 582–589. 1976.

3. *Chernov G.P.* Whistlers in the solar corona and their relevance to fine structures of type IV radio emission // Sol. Phys. V. 130. N 1–2. P. 75–82. 1990. https://doi.org/10.1007/BF00156780

4. *Chernov G.P.* A manifestation of quasilinear diffusion in whistlers in the fine structure of type IV solar radio bursts // Astron. Rep. V. 40. N 4. P. 561–568. 1996.

5. *Chernov G.P.* The relationship between fine structure of the solar radio emission at meter wavelengths and coronal transients // Astron. Lett. V. 23. N 6. P. 827–837. 1997.
6. *Chernov G.P.* Solar radio burst with drifting stripes in emission and absorption // Space Sci. Rev. V. 127. N 1–4. P. 195–326. 2006. https://doi.org/10.10007/s11214-006-9141-7
7. *Chernov G.P., Stanislavsky A.A., Konovalenko A.A., Abranin E. P., Dorovsky V. V., Rucker H.O.* Fine structure of decametric type II radio bursts // Astron. Lett. V. 33. N 3. P. 192–202. 2007. https://doi.org/10.1134/S1063773707030061
8. *Chernov G.P.* Manifestation of quasilinear diffusion on whistlers in the fine structure radio sources of solar radio bursts // Plasma Phys. Rep. V. 31. N 4. P. 314–324. 2005. https://doi.org/10.1134/1.1904148
9. *Chernov G.P.* Unusual stripes in emission and absorption in solar radio bursts: Ropes of fibers in the meter wave band // Astron. Lett. V. 34. N 7. P. 486–499. 2008. https://doi.org/10.1134/S1063773708070074
10. *Chernov G.P.* Fine structure of solar radio bursts. Heidelberg: Springer, 282 p. 2011. https://doi.org/10.10007/978-3-642-20015-1
11. *Chernov G.P.* Latest data on the fine structure in solar radio emission / LAMBERT Academic Publisher. Riga, Latvia, 284 p. 2019.
12. *Chernov G.P., Fomichev V.V., Sych R.A.* A model of zebra patterns in solar radio emission // Geomagn. Aeronomy. V. 58. N 3. P. 394–406. 2018. https://doi.org/10.1134/S0016793218030040
13. *Elgarøy Ø.* Observations of the fine structure of enhanced solar radio radiation with a narrow-band spectrum analyser // Nature. V. 184. N 4690. P. 887–888. 1959. https://doi.org/10.1038/184887a0
14. *Fomichev V.V., Fainstein S.M., Chernov G.P.* A possible interpretation of the zebra pattern in solar radiation // Plasma Phys. Rep. V. 35. N 12. P. 1032–1035. 2009. https://doi.org/10.1134/S1063780X09120058
15. *Karlický M., Bárta M., Jiřička K., Meszárosová H., Sawant H.S., Fernandes F. C.R., Cecatto J.R.* Radio bursts with rapid frequency variations – lace bursts // Astron. Astrophys. V. 375. N 2. P. 638–642. 2001. https://doi.org/10.1051/0004-6361:20010888
16. *Karlický M.* Radio continua modulated by waves: Zebra patterns in solar and pulsar radio spectra // Astron. Astrophys. V. 552. ID A90. 2013. https://doi.org/10.1051/0004-6361/201321356
17. *Karlický M*. Frequency variations of solar radio zebras and their power-law spectra // Astron. Astrophys. V. 561. ID A34. 2014. https://doi.org/10.1051/00046361/201322547
18. *Karlický M.* Simulations of the solar radio zebra // Astron. Astrophys. V. 661. ID A56. 2022. https://doi.org/10.1051/0004-6361/202142497

19. *Kuijpers J.* Collective wave-particle interactions in solar type IV radio sources. Ph.D. Thesis. Utrecht, The Netherlands: Utrecht University. 72 p. 1975.
20. *Kuijpers J.* Theory of type IV dm Bursts // Symposium - International Astronomical Union. V. 86. P. 341–361. 1980. https://doi.org/10.1017/S0074180900037098
21. *Kuznetsov A.A., Tsap Yu.T.* Loss-cone instability and formation of zebra patterns in type IV solar radio bursts // Sol. Phys. V. 241. P. 127–148. 2007. https://doi.org/10.1007/S11207-006-0351-7
22. *LaBelle J., Treumann R.A., Yoon P.H., Karlický M.* A model of zebra emission in solar type IV radio bursts // Astrophys. J. V. 593. N 2. P. 1195–11207. 2003. https://doi.org/10.1086/376732.
23. *Laptuhov A.I., Chernov G.P.* New mechanism for the formation of discrete stripes in the solar radio spectrum // Plasma Phys. Rep. V. 32. N 10. P. 866–871. 2006. https://doi.org/10.1134/S1063780X06100060
24. *Laptuhov A.I., Chernov G.P.* Concerning mechanisms for the zebra pattern formation in the solar radio emission // Plasma Phys. Rep. V. 35. N 2. P. 160–168. 2009. https://doi.org/10.1134/S1063780X09020081
25. *Litvinenko G.V., Shaposhnikov V.E., Konovalenko A.A., Zakharenko V.V., Panchenko M., Dorovsky V.V., Brazhenko A.I., Rucker H.O., Vinogradov V.V., Melnik V.N.* Quasi-similar decameter emission features appearing in the solar and jovian dynamic spectra // Icarus. V. 272. P. 80–87. 2016. https://doi.org/10.1016/j.icarus.2016.02.039
26. *Mollwo L.* Interpretation of patterns of drifting zebra stripes // Sol. Phys. V. 83. N 2. P. 305–320. 1983. https://doi.org/10.1007/BF00157482
27. *Mollwo L.* The magneto-hydrostatic field in the region of Zebra patterns in solar type-IV dm-bursts // Sol. Phys. V. 116. N 2. P. 323–348. 1988. https://doi.org/10.1007/BF00157482
28. *Panchenko M, Rošker S., Rucker H.O. et al.* Zebra pattern in decametric radio emission of Jupiter // Astron. Astrophys. V. 610. ID A69. 2018. https://doi.org/10.1051/0004-6361/201731369
29. *Selhorst C.L., Silva-Válio A., Costa J.E.R.* Solar atmospheric model over a highly polarized 17 GHz active region // Astron. Astrophys. V. 488. N 3. P. 1079–1084. 2008. https://doi.org/10.1051/0004-6361:20079217
30. *Slottje C.* Peculiar absorption and emission microstructures in the type IV solar radio outburst of March 2, 1970 // Sol. Phys. V. 25. N 1. P. 210–231. 1972. https://doi.org/10.1007/BF00155758
31. *Slottje C.* Atlas of fine structures of dynamics spectra of solar type IV-dm and some type II radio bursts. Utrecht, The Netherlands: Dwingeloo Observatory, 233 p. 1981.
32. *Treumann R.A., Gudel M., Benz A.O.* Alfven wave solitons and solar intermediate drift bursts // Astron. Astrophys. V. 236. N 1. P. 242–249. 1990.

33. *Viktorov M., Mansfeld D., Golubev S.* Laboratory study of kinetic instabilities in a nonequilibrium mirror-confined plasma // Europhys. Lett. V. 109. N 6. ID 65002. 2015. https://doi.org/10.1209/0295-5075/109/65002
34. *Winglee R.M. and Dulk G.A.* The electron-cyclotron maser instability as a source of plasma emission // Astrophys. J. V. 307. P. 808–819. 1986. https://doi.org/10.1086/164467
35. *Yasnov L.V., Chernov G.P.* Alternative models of zebra patterns in the event on June 21, 2011 // Sol. Phys. V. 295. N 2. ID 13. 2020. https://doi.org/10.1007/s11207-020-1585-5
36. *Yasnov L.V., Karlický M., Stupishin A.G.* Physical conditions in the source region of a zebra structure // Sol. Phys. V. 291. N 7. P. 2037–2047. 2016. https://doi.org/10.1007/s11207-016-0952-8
37. *Yasnov L.V., Karlický M.* Magnetic field, electron density and their spatial scales in zebra pattern radio sources // Sol. Phys. V. 295. N 7. ID 96. 2020. https://doi.org/10.1007/s11207-020-01652-w
38. *Zheleznyakov V.V., Zlotnik E.Ya*. Cyclotron wave instability in the corona and origin of solar radio emission with fine structure // Sol. Phys. V. 43. N 2. P. 431–451. 1975a. https://doi.org/10.1007/BF00152366
39. *Zheleznyakov V.V., Zlotnik E.Ya.* Cyclotron wave instability in the corona and origin of solar radio emission with fine structure. III. Origin of zebra pattern // Sol. Phys. V. 44. N 2. P. 461–470. 1975b. https://doi.org/10.1007/BF00153225
40. *Zheleznyakov V.V., Zlotnik E.Ya., Zaitsev V.V., Shaposhnikov V.E*. Double plasma resonance and its manifestations in radio astronomy // Phys.-Usp. V. 59. N 10. P. 997–1120. 2016. https://doi.org/10.3367/UFNe.2016.05.037813
41. *Zlotnik E.Ya., Zaitsev V.V., Aurass H., Mann G., Hofmann A.* Solar type IV burst spectral fine structures. II. Source model // Astron. Astrophys. V. 410. N 3. P. 1011–1022. 2003. https://doi.org/10.1051/0004-6361:20031250
42. *Zlonik E.Ya., Zaitsev V.V., Aurass H., Mann G.A*. Special radio spectral fine structure used for plasma diagnostics in coronal magnetic traps // Sol. Phys. V. 255. N 2. P. 273–288. 2009. https://doi.org/10.1007/s11207-009-9327-8
43. *Zlotnik E.Y., Shaposhnikov V.E., Zaitsev V.V.* Interpretation of the zebra pattern in the Jovian kilometric radiation // J. Geophys. Res. – Space. V. 121. N 6. P. 5307–5318. 2016. https://doi.org/10.1002/2016JA022655

FIGURE CAPTIONS

Fig. 1. Complex zebra structure from IZMIRAN spectrograph data in the 180-270 MHz range in the July 18, 2000 phenomenon.

Fig. 2. Complex event of 01.12.2004 with smooth transition of fibers (fiber bursts) into zebra bands with sawtooth frequency drift in the range 1.1-1.34 GHz (Huairou station, National Astronomical Observatory of China (NAOC)) in the 01.12.2004 event.

Fig. 3. (*a*) Harmonics of the cyclotron frequency $s\omega_{Be}$ and plasma frequency ω_{Pe} as a function of the coordinate x for characteristic scales of variation of the magnetic field LB and density LN at $|LB| < |$ LN| (fragment of Fig. 2 from [Zheleznyakov et al., 2016]);

(*b*) Electron density profile as a function of height h in the solar atmosphere according to [Selhorst et al., 2008]).

Fig. 4. Altitude dependence of the plasma frequency according to the barometric law (bold line) and altitude profiles of electron cyclotron harmonic s (thin lines) in the solar corona. For electron temperature $T_e = 1.2\text{-}10^6$ K and initial frequency f_{P0} = 3800 MHz at altitude h_{B0} = 20 000 km, 34 DPR levels are formed in the corona between plasma levels 2600-3800 MHz (from [Laptuhov and Chernov, 2009]).

Fig. 5. Dynamic spectrum of the plasma emission. The types of kinetic instabilities considered in the paper are distinguished: 1) the initial stage of ESR discharge (sparse plasma); 2 and 3) stages of developed discharge (dense plasma); 4) the initial phase of plasma decay (dense plasma); 5) decaying plasma (sparse plasma). Three lines on the spectrogram show the time variation of the corresponding frequencies $2f_{ce0}$, f_{ce0} and $1/2f_{ce0}$, where $f_{ce0} \equiv f_{ce}$ − electron cyclotron frequency at the center of the magnetic trap on its axis. ECR heating switch-of - turning off the electron cyclotron resonance heating.

(fragment of Fig. 2 from [Viktorov et al., 2015]). We note the strict periodicity of whistler generation.

Fig. 6. Example of a WSO in the radio emission of Jupiter, observed with the Ukrainian radio telescope URAN-2, January 30, 2014. Fragment of Fig. 1 from [Panchenko et al., 2018].

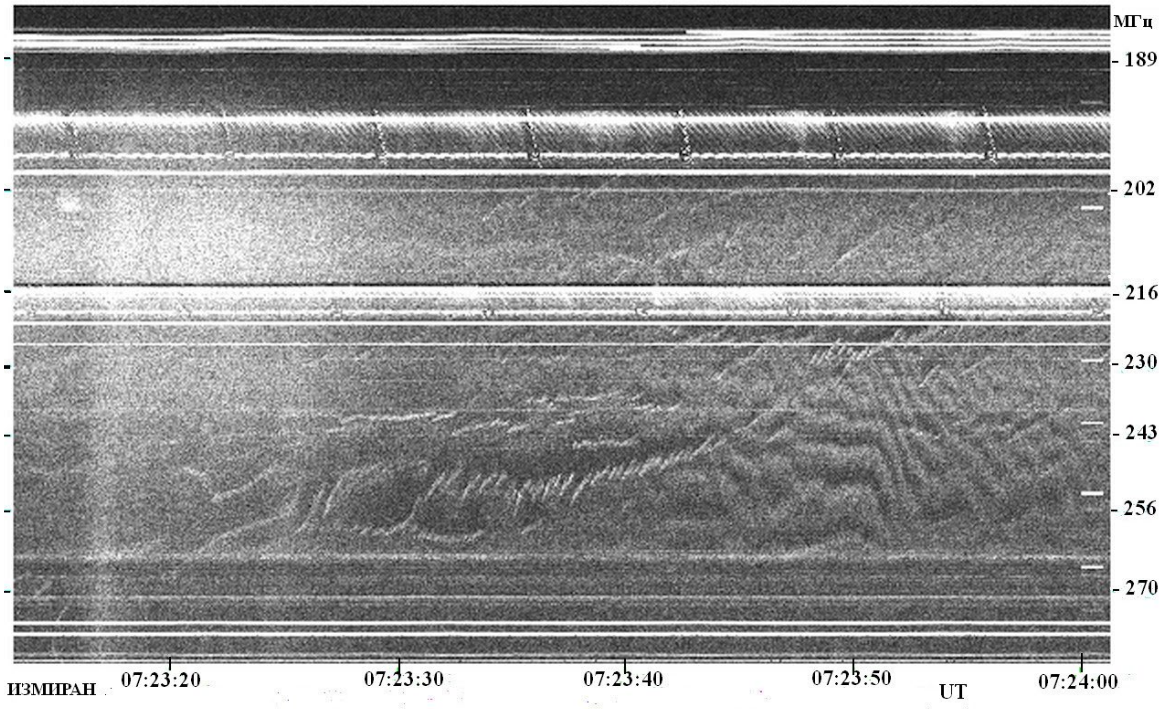
МГц
189
202
216
230
243
256
270
ИЗМИРАН
07:23:20
07:23:30
07:23:40
07:23:50
UT
07:24:00

Fig. 1.

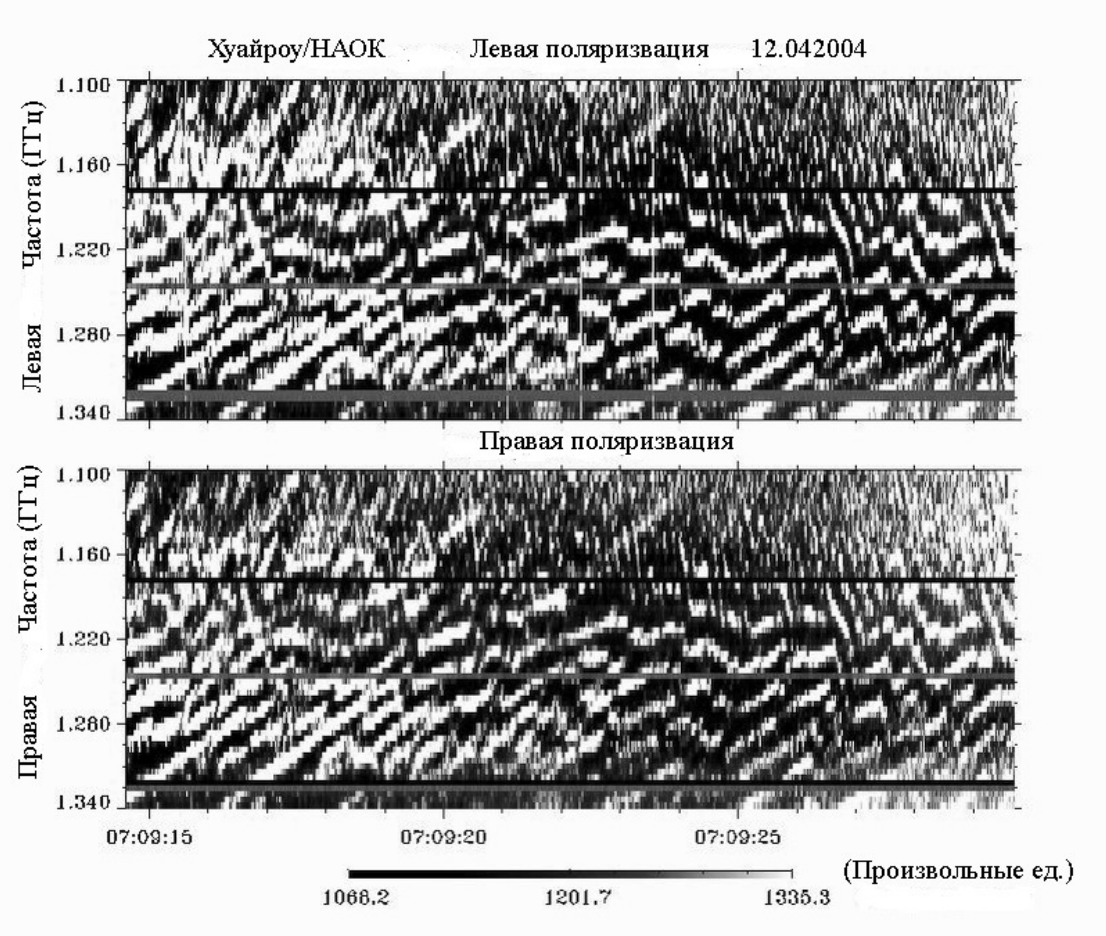
Хуайроу/НАОК
Левая поляризвация
12.042004
Частота (ГГц)
Левая
1.100
1.160
1.220
1.280
1.340
Правая поляризвация
Частота (ГГц)
Правая
1.100
1.160
1.220
1.280
1.340
07:09:15
07:09:20
07:09:25
(Произвольные ед.)
1066.2
1201.7
1335.3

Fig. 2.

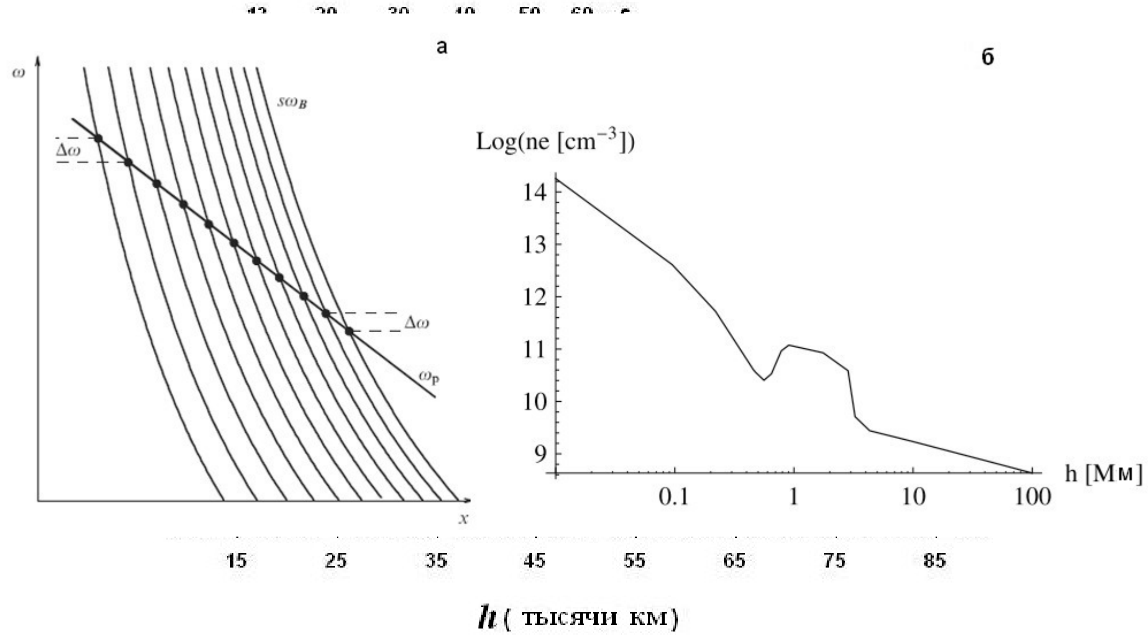
а
б
ω
sω_B
Δω
Δω
ω_p
x
Log(ne [cm^-3])
14
13
12
11
10
9
0.1
1
10
100
h [Мм]
15
25
35
45
55
65
75
85
h (тысячи км)

Fig. 3.

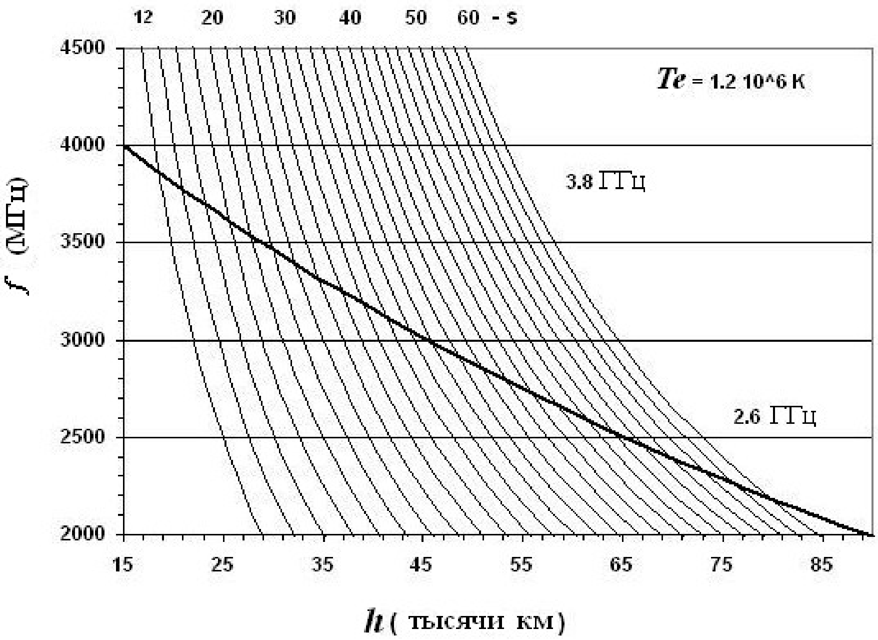

12
20
30
40
50
60 - s
Te = 1.2 10^6 K
3.8 ГГц
2.6 ГГц
f (МГц)
4500
4000
3500
3000
2500
2000
15
25
35
45
55
65
75
85
h (тысячи км)

Fig. 4.

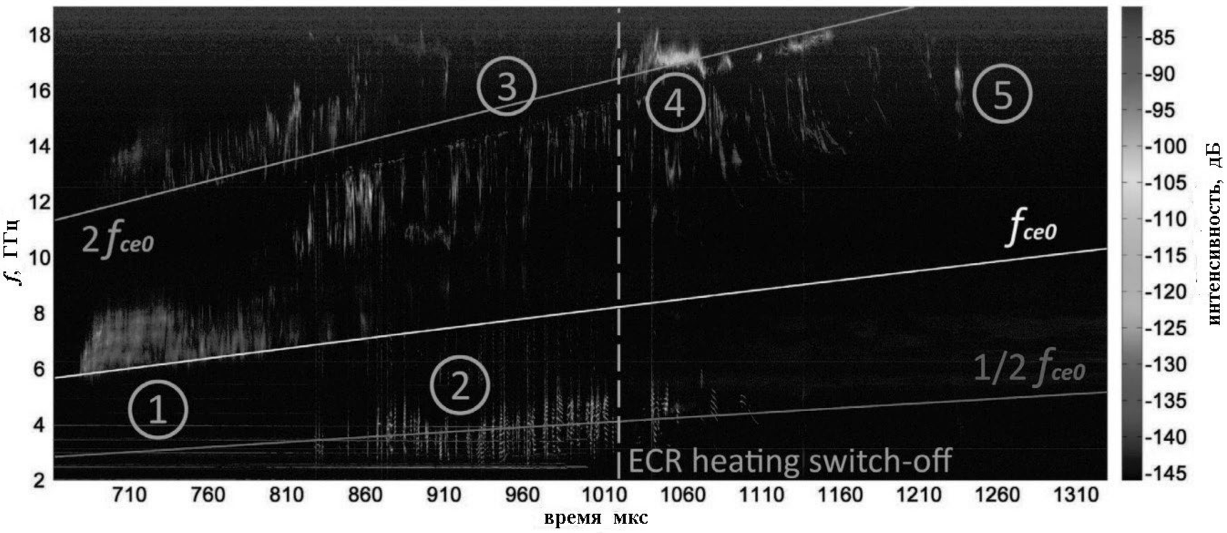

18
16
14
12
10
8
6
4
2
f, ГГц
710
760
810
860
910
960
1010
1060
1110
1160
1210
1260
1310
время мкс
-85
-90
-95
-100
-105
-110
-115
-120
-125
-130
-135
-140
-145
интенсивность, дБ
$2f_{ce0}$
f_{ce0}
$1/2\,f_{ce0}$
1
2
3
4
5
ECR heating switch-off

Fig. 5.

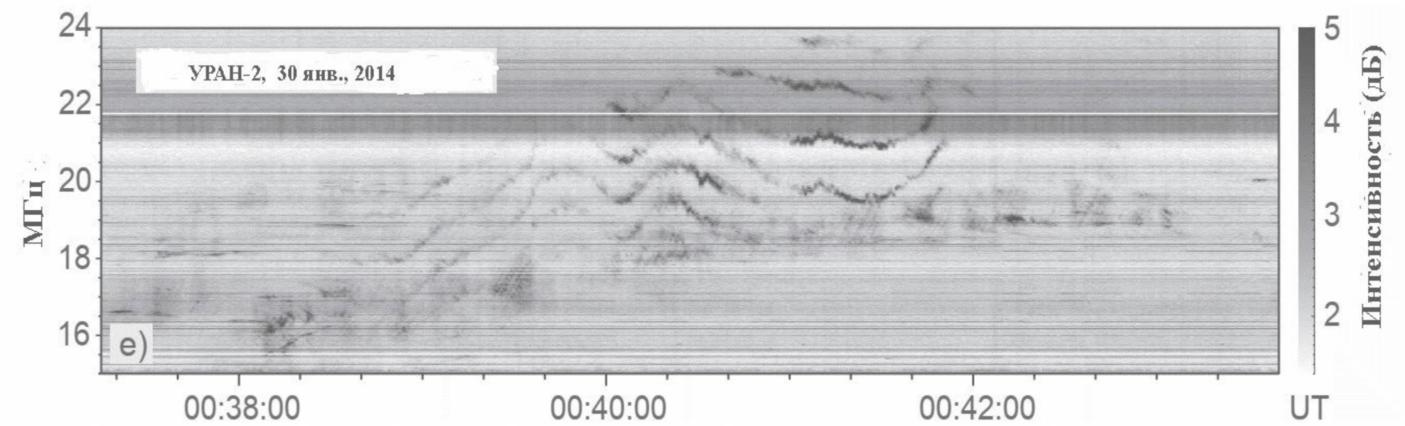

УРАН-2, 30 янв., 2014
МГц
Интенсивность (дБ)
e)
24
22
20
18
16
00:38:00
00:40:00
00:42:00
UT
5
4
3
2

Fig. 6.